

Document downloaded from:

<http://hdl.handle.net/10251/183254>

This paper must be cited as:

García Martínez, A.; Monsalve-Serrano, J.; Villalta-Lara, D.; Guzmán-Mendoza, MG. (2021). Methanol and OME_x as fuel candidates to fulfill the potential EURO VII emissions regulation under dual-mode dual-fuel combustion. *Fuel*. 287:1-13.
<https://doi.org/10.1016/j.fuel.2020.119548>



The final publication is available at

<https://doi.org/10.1016/j.fuel.2020.119548>

Copyright Elsevier

Additional Information

1 **Methanol and OME_x as fuel candidates to fulfill the potential EURO VII emissions**
2 **regulation under dual-mode dual-fuel combustion**

3 **Antonio García^{*}, Javier Monsalve-Serrano, David Villalta and María Guzmán-**
4 **Mendoza**

5 **Fuel, Volume 287, 1 March 2021, 119548**
6 **<https://doi.org/10.1016/j.fuel.2020.119548>**

7 CMT - Motores Térmicos, Universitat Politècnica de València, Camino de Vera s/n,
8 46022 Valencia, Spain

9
10 Corresponding author (*):

11 Dr. Antonio García (angarma8@mot.upv.es)

12 Phone: +34 963876574

13 Fax: +34 963876574

14
15 **Abstract**

16 Recent investigations show that there are different combustion strategies that promise
17 to achieve higher efficiencies in internal combustion engines. Advanced combustion
18 modes such as reactivity controlled compression ignition (RCCI) and dual-mode dual-
19 fuel (DMDF) have proven to be able to achieve low NO_x and soot engine-out emissions
20 while being able to operate over the complete engine map. On another front, intensive
21 research has been done in the fuels field. Oxygenated fuels, like oxymethylene dimethyl
22 ethers (OME_x) and methanol, are of special interest because of their potential to reduce
23 the soot emissions, while allowing to adjust parameters, such as EGR, to higher values
24 to also reduce NO_x emissions and avoid other problems like excessive in-cylinder peaks
25 of pressure. In this research, the effects of diesel-methanol and OME_x-gasoline fuels
26 were studied on a dual-mode dual-fuel (DFDM) multi-cylinder engine at 1800 rpm for
27 various loads (25, 50, 80 and 100%). To do so, a dedicated calibration to optimize the
28 brake thermal efficiency while trying to maintain NO_x and soot emissions under EURO
29 VI limitations was applied. Then, the combustion characteristics, performance and
30 emissions results are compared to a base diesel-gasoline case. Boundary conditions
31 (intake pressure, temperature and air mass) for each fuel combination were similar,
32 with the exception of the premixed energy ratio, which was on average 20% lower for
33 diesel-methanol. Each fuel combination was, weighted against each other by means of
34 an merit function, where the fuel combination with the lowest value has the closest
35 approximation to ideal BSFC_{eq}, BSNO_x, BSSoot, BSCO and BSHC targets. Results show
36 that diesel-methanol presents no significant differences with respect to diesel-gasoline
37 in terms of equivalent BSFC_{eq} and NO_x, while the substitution of diesel by OME_x in the
38 dual-mode dual-fuel combustion has the potential of, although penalizing HC and CO
39 emissions, not only achieving the EURO VI NO_x (0.4 g/kWh) limits but also the future
40 potential EURO VII (0.2 g/kWh) as well because of a negligible soot production that
41 allows using EGR levels of up to 50%.

42 **Keywords**

43 Dual fuel combustion; OME_x; Methanol; e-Fuels; EUVII emissions

44

45 1. Introduction

46 Emissions regulations must evolve through time and become stricter to try to
47 mitigate the steep increase of greenhouse gases emissions and pollution because of the
48 negative effects that they have on human health [1] and the environmental wear that
49 they cause [2]. Regulations are a way to, firmly, incentivize manufacturers to develop
50 new strategies in order to avoid environmental pollution and emissions . The transport
51 sector has an important contribution to these emissions; in Europe, this sector makes
52 up almost a quarter of the Greenhouse gases and is the main cause of pollution in the
53 cities [3]. Although electric vehicles are generally considered cleaner on per use
54 emissions and, as such a solution to the reduction of emissions and compliance with
55 regulations, they are not exempt from polluting the air [4]. Therefore, is in the best
56 interest of the automotive industry to continue researching and improving the internal
57 combustion engine (ICE) technology to fulfill the new restrictions. Especially, since ICE
58 vehicles are expected to be the main source of transportation in the foreseeable future
59 [5].

60 Recently, several investigations on the engine hardware [6] [7], combustion
61 concepts [8] [9], and electric powertrain coupling [10] [11] have made considerable
62 progress in achieving the objectives of reducing emissions without penalizing the
63 performance. However, these advancements by themselves will not be enough in the
64 long term. To aid in this task the development and investigation of new fuels, and
65 strategies to use such fuels in a way that enables the combustion engines to take
66 advantage of most of the energy available, is of the utmost importance. In this regard,
67 new fuels have appeared with properties like better more oxygenation [12] [13], carbon
68 neutrality [14], more energy content or electrical recharge ability [15]. Highly
69 oxygenated fuels like methanol and OME_x are interesting case studies to appreciate the
70 enhancements and downsides that their properties contribute when used coupled with
71 combustion concepts like reactivity controlled compression ignition (RCCI) and dual-fuel
72 dual-mode (DFDM) [8] [16]; thus, they will be the focus of this paper.

73 Previous research has indicated that using oxygenated fuels, like methanol and
74 OME_x, can effectively reduce the soot formation in compression ignition (CI) engines
75 [17] [18]. Methanol, in particular, has been considered as a replacement for
76 conventional diesel because it burns at lower temperatures, producing, in principle, less
77 NO_x [19]. It is a single carbon renewable fuel that can be produced in different ways:
78 from fossil fuels, biomass and carbon capture and utilization schemes (the latter two,
79 both renewable energy sources) [20]. It has a higher oxygen content, enthalpy of
80 vaporization and octane number than gasoline, characteristics that can enhance
81 reactivity gradients and extend the operational load range [21]. Its simpler molecular
82 structure reduces the formation of soot [22], as the fuel reacts faster with oxygen, of
83 which it has a higher content. In this study, methanol is used as the low reactivity fuel
84 (LRF) for a DFDM concept in tandem with diesel as the high reactivity fuel (HRF). Several
85 studies using methanol as an additive for diesel or as a blend [23] [24], found that smoke,
86 CO and unburned HC emissions are decreased, but NO_x increased as the methanol
87 proportion in the blend increased. Works on low temperature combustion (LTC) modes
88 with methanol, although scarcer, can also be found. In [25], Li et al. studied the
89 optimization of diesel-methanol at low loads with RCCI and direct dual fuel stratification
90 (DDFS), [26] compared diesel-methanol and PODE-methanol fuels in RCCI combustion

91 and [27] also researched methanol for RCCI by both direct injection (DI) and port
92 injection, finding that it has the potential of achieving ultra-low NO_x through port
93 injection.

94 On the other hand, Oxymethylene dimethyl ethers (OMEx) are a family of synthetic
95 fuels formed by the chemical structure CH₃O(CH₂O)_xCH₃ where x can take values from 1
96 to 5 [28], modifying the size of the molecule. The larger molecules (x=3-5) can be used
97 for compression-ignition engines due to their very high cetane numbers [14]. These e-
98 fuels lack C-C bonds and possess many oxygen atoms, which promote negligible soot
99 emissions [29]. Methanol and formaldehyde are intermediate steps in its production
100 [30] and the synthetization process demands lower electrical energy for its production
101 than other e-fuels [29]. Previously, OMEx used as a HRF with gasoline as a LRF has been
102 compared to diesel-gasoline in dual-fuel combustion [31] [32] [33], resulting in ultra-low
103 soot values throughout all the engine map. The low soot values allowed to calibrate the
104 engine to also have high EGR levels, that reduce NO_x emissions, and higher efficiency
105 due to lower pumping losses.

106 This work, aims to compare the combustion, performance and emissions of diesel-
107 methanol and OMEx-gasoline under DFDM, on a multi-cylinder engine working at 1800
108 rpm and 25, 50, 80 and 100% load to evaluate if they have the potential to reduce
109 emissions (NO_x and soot) while maintaining performance to fulfill EURO VI emission
110 limits and beyond (EU VII) without significantly increasing fuel consumption nor the
111 requirements for aftertreatment systems.

112 **2. Materials and methods**

113 The following section outlines the steps followed and the equipment employed
114 during the investigation. In particular, the engine, test facilities and the trial procedures
115 will be presented.

116 **2.1. Engine characteristics**

117 Tests were performed in a multi-cylinder, four stroke, 8L, compression ignition
118 engine modified to be able to operate under a dual-fuel combustion strategy. Among its
119 modifications from the commercially available unit, six port fuel injectors (PFI) were
120 installed to inject the low reactivity fuel (LRF) in the intake manifold. Moreover, to avoid
121 excessive peak pressure gradients at high loads, the compression ratio (CR) was reduced
122 from 17.5:1 to 12.8:1. To do so, the piston bowl was optimized to be more compatible
123 with the RCCI mode. Finally, a low pressure (LP) exhaust gas recirculation (EGR) system
124 was added to deliver EGR and maintain the mass flow in the turbine, whilst lowering the
125 temperature of the EGR gasses. Table 1 describes the engine main characteristics.

126

127

128

129

130

131

132

Table 1. Engine characteristics.

Engine Type	4 stroke, 4 valves, direct injection
Number of cylinders [-]	6
Displaced volume [cm ³]	7700
Stroke [mm]	135
Bore [mm]	110
Piston bowl geometry [-]	Bathtub
Compression ratio [-]	12.75:1
Rated power [kW]	235 @ 2100 rpm
Rated torque [Nm]	1200 @ 1050-1600 rpm

133

134

2.2. Description of the test cell

135

136

137

138

139

140

141

142

143

The main measurement devices are represented in the test cell facility scheme (Figure 1). Fully premixed combustion requires a high level of charge dilution, for this, a LP EGR system was incorporated to the stock engine. Additional water filters were included before the compressor to remove the water condensates formed in the EGR line caused by the temperature drop [35]. The average values for temperature and pressure were recorded at the locations represented in the scheme shown in Figure 1. A Kistler 6125C cylinder pressure transducer was equipped to each individual cylinder to allow the detection of possible cylinder-to-cylinder dispersions on the different gaseous quantities: air, EGR and LRF.

144

145

146

147

148

149

150

151

152

153

154

155

156

157

158

159

The data was collected using an AVL 364 encoder with a of 0.2 crank angle degree (CAD) resolution. A Horiba MEXA-7100 DEGR analyzer measured the O₂, CO, CO₂, NO_x and HC at the exhaust. To quantify the smoke emissions by extracting a subset of the exhaust gas and passing it through a filter paper, an AVL 415S smoke meter was used. With this device, the blackening of the filter paper indicates the soot content in its own unit filter smoke number (FSN) [34]. Instantaneous fuel consumption for both the HRF and LRF was measured by two AVL 733 S balances. Air mass flow was measured with an Elster RVG G100 sensor. An AVL PUMA interface was utilized for the acquisition of low frequency data, at a rate of 10 Hz, and controlling the engine speed. Engine torque was user regulated. A NI PXIe 1071 board controlled all injection systems (high reactivity and low reactivity) and recorded high frequency signals; it was able to process pressure data and perform a heat release analysis in real time. The board allows the monitoring of the main combustion metrics and heat release rate (HRR) profile while connected to a controller system developed in the research facility. It also allows the control of the back-pressure valve and the LP EGR system. Table 2 displays the main elements of the test cell with their respective accuracy.

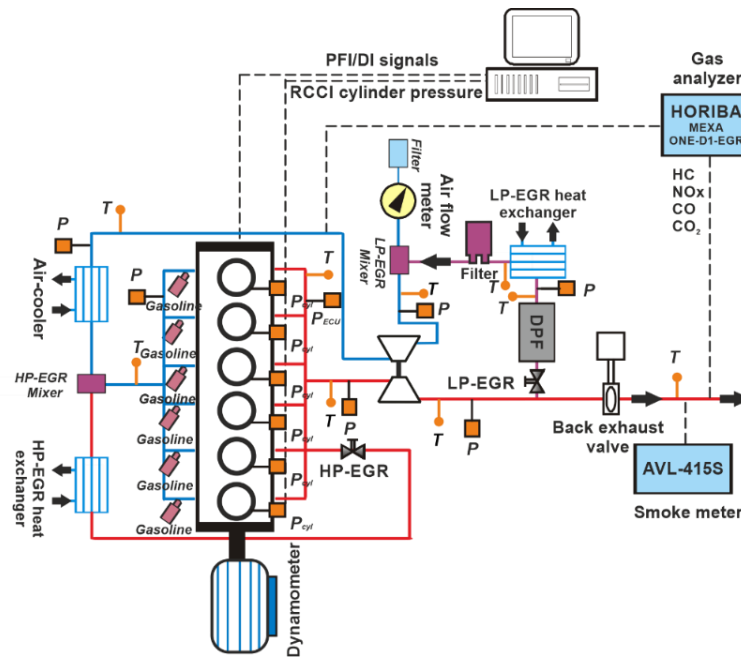


Figure 1. Test cell scheme.

Table 2. Instrumentation information.

Variable measured	Device	Manufacturer / model	Accuracy
In-cylinder pressure	Piezoelectric transducer	Kistler / 6125C	± 1.25 bar
Intake/exhaust pressure	Piezoresistive transducers	Kistler / 4045A	± 25 mbar
Temperature in settling chambers and manifolds	Thermocouple	TC direct / type K	± 2.5 °C
Crank angle, engine speed	Encoder	AVL / 364	± 0.02 CAD
NOx, CO, HC, O ₂ , CO ₂	Gas analyzer	HORIBA / MEXA 7100 DEGR	4%
FSN	Smoke meter	AVL / 415	± 0.025 FSN
Gasoline/diesel fuel mass flow	Fuel balances	AVL / 733S	$\pm 0.2\%$
Air mass flow	Air flow meter	Elster / RVG G100	$\pm 0.1\%$

2.3. Fuels and injection systems characteristics

Dual-fuel configurations require injection systems adapted to the premise of having to inject both a high reactivity fuel (HRF) and a low reactivity one. This research focuses on OMEx-Gasoline (OMEx-G) and diesel-methanol as the main fuel combinations to perform analysis on. The characteristics of the fuels discussed are described in Table 3.

Table 3. Fuel physical and chemical properties.

	EN 228 gasoline	EN 590 diesel	Methanol	OMEx
Density [kg/m ³] (T= 15 °C)	720	842	792	1067
Viscosity [mm ² /s] (T= 40 °C)	0.545	2.929	0.58	1.18
Cetane number [-]	-	55.7	-	72.9
Carbon content [% m/m]	-	86.2	-	43.6
Hydrogen content [% m/m]	-	13.8	-	8.82
Oxygen content [% m/m]	-	0	-	47.1
RON [-]	95.6	-	109	-
MON [-]	85.7	-	100	-
Lower heating value [MJ/kg]	42.4	42.44	19.93	19.04

176

177 As previously mentioned, a PFI system was adapted to the engine to be able to inject
 178 the LRF (gasoline or methanol); said system operates at 5.5 bar. The stock injection
 179 system was used to inject the HRF (OMEx, in the case of OMEx-G tests, and diesel, for
 180 diesel gasoline tests)through direct injection (DI). The same Labview software controlled
 181 the injection timing and fuel mass for both the HRF and LRF. Table 4 describes the most
 182 important information of the fuel injection systems used in the research facility.

183

Table 4. Characteristics of the direct and port fuel injectors.

Direct injector		Port fuel injector	
Actuation Type [-]	Solenoid	Injector Style [-]	Saturated
Steady flow rate @ 100 bar [cm ³ /min]	1300	Steady flow rate @ 3 bar [cm ³ /min]	980
Included spray angle [°]	150	Included Spray Angle [°]	30
Number of holes [-]	7	Injection Strategy [-]	single
Hole diameter [µm]	177	Start of Injection [CAD ATDC]	340
Maximum injection pressure [bar]	2500	Maximum injection pressure [bar]	5.5

184

185 2.4. Calibration methodology description

186 Implementation of a dedicated calibration methodology was done to stay within
 187 predefined constraints, i.e. the upper exhaust pressure limit imposed by the size of the
 188 turbocharger. A multiple-injection strategy was used to allow more degrees of freedom
 189 controlling the combustion and, therefore, achieving the desired targets. The first
 190 calibration step sought to achieve the desired load operating under dual-fuel conditions
 191 while maintaining the pressure gradient under 15 bar/CAD and the maximum pressure
 192 below 185 bar. For that purpose, the engine was started at conventional diesel
 193 combustion (CDC) conditions. Then, the LRF percentage was incremented to reach the
 194 maximum premixed energy ratio (PER); this step was iterated over after the last step of
 195 the calibration loop. Higher PER values indicate that the LRF governs the combustion
 196 process and excessive pressure rise rates (PRR) and high cylinder pressure can be seen.
 197 Consequently, to avoid mechanical problems it is necessary to decrease the PER by
 198 delaying the start of injection (SOI) of the HRF, attempting to shift the injection towards
 199 after top dead center (TDC). Finally, the indicated mean effective pressure coefficients
 200 of variations are targeted to values lower than 4% to procure a stable combustion. When

201 the load was accomplished, and all the constraints are satisfied, the next step was
202 commenced.

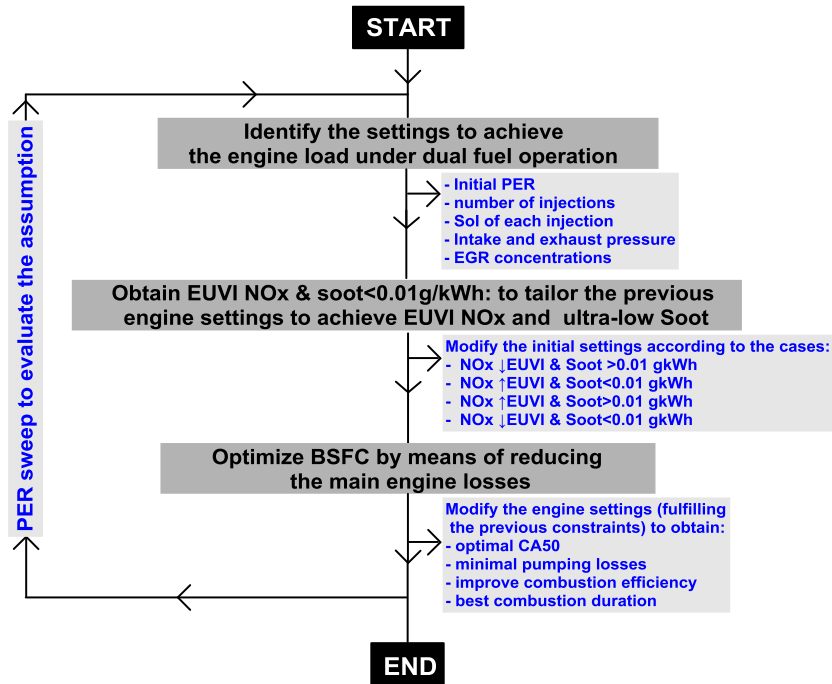
203 The successive phase involves the compliance with the regulations of EURO VI for
204 soot and NO_x. To comply with EURO VI regulations for particulate matter (PM) of soot,
205 a limit of 0.01 g/kWh was imposed. The limit is intended to ensure the quantity of PM
206 emissions are below EURO VI; however, it does not ensure that soot (in terms of PM)
207 will be below EURO VI. It does guarantee tests with soot contents above this limit will
208 also be uncompliant wit EURO VI. After the load setting step, four different scenarios
209 can be presented: either NO_x and soot are below (0.4 g/kWh and 0.01 g/kWh
210 respectively), NO_x is below EUVI limit and soot is above 0.01 g/kWh, NO_x is over the
211 EUVI limit and soot is below 0.01 g/kWh, or both pollutants exceed the limits.

212 Depending on the aforementioned scenarios, different methods are recommended
213 to reach the limit values. If NO_x are higher than EUVI, there are several alternatives to
214 follow: 1) increase the EGR concentration to increment the dilution levels, 2) shift the
215 combustion closer to the compression stroke by delaying the SOI in order to reduce the
216 temperatures during the combustion. Otherwise, when soot values are higher than the
217 specified limit, the in-cylinder oxygen concentration should be increased and the
218 mixture improved. This can be done with higher injection pressures aimed at improving
219 the penetration and evaporation sprays; reducing the EGR concentration and increasing
220 the degree of dilution; increasing the inlet pressure; and using earlier SOIs to promote
221 longer mixing times thereby reducing the zone-rich equivalence ratio.

222 High load conditions have a bigger chance of exceeding both NO_x and soot limits,
223 because part of the HRF burns diffusively and the more elevated temperatures favor the
224 NO_x formation. Strategies must therefore be used to reduce NO_x and soot, such as
225 increasing the EGR concentration, increasing the oxygen concentration at the intake (by
226 closure of the turbine), moving SOI forward to an earlier stage and increasing the
227 injection pressure. These strategies usually have adverse effects on soot and NO_x;
228 increasing EGR could reduce the NO_x but enhance the soot formation due to the
229 decrease of the air to fuel equivalence ratio, and earlier SOIs and injection pressure
230 could lead to higher in-chamber temperatures and the subsequent increase in NO_x
231 formation. Hardware flexibility is explored to achieve emission target, however, when
232 this cannot be done, constraints can be set to less strict parameters to reach the desired
233 engine load.

234 The final step of the calibration aims to reduce the main losses that occur during the
235 conversion of the chemical energy from the fuel into mechanical energy, while
236 maintaining the emission limits achieved in the previous step. In order to provide the
237 required amount of EGR and reduce pumping losses, the position of the variable
238 geometry turbine (VGT) is modified; then, a sweep of the LP and HP EGR is made, while
239 also varying the VGT position to provide the same amount of air and EGR, but with a
240 better turbine efficiency and lower backpressure in the engine. The other processes of
241 this step aim to achieve optimal combustion phasing, improved combustion efficiency
242 and minimal pumping losses by evaluating the effect of small modifications on the PER,
243 SOI and EGR.

244 Figure 2 presents a scheme of the calibration methodology steps presented above.
 245 To ensure the calibration does not coincide with a local minimum, and that the initial
 246 high PER assumption is true, the PER is evaluated again at the end of the loop.



247
 248 Figure 2. Engine calibration loop for each fuel blend.

249 Because this work compares different fuels, with significantly different lower heating
 250 values (LHV), fuel consumption results are compared on an equivalent basis. The
 251 selection of this method seeks to evaluate the conversion efficiency of the fuels and
 252 exclude the impact of the LHV. This is done by defining the equivalent brake specific fuel
 253 consumption ($BSFC_{eq}$) using the lower heating value of diesel as reference, and
 254 accounting for the fuels in terms of mass and their respective LHV.

$$BSFC_{eq} [g/kWh] = \frac{\dot{m}_{HRF} \cdot \left(\frac{LHV_{HRF}}{LHV_{diesel}} \right) + \dot{m}_{LRF} \cdot \left(\frac{LHV_{LRF}}{LHV_{gasoline}} \right)}{P_b} \quad (1)$$

255 3. Results and discussion

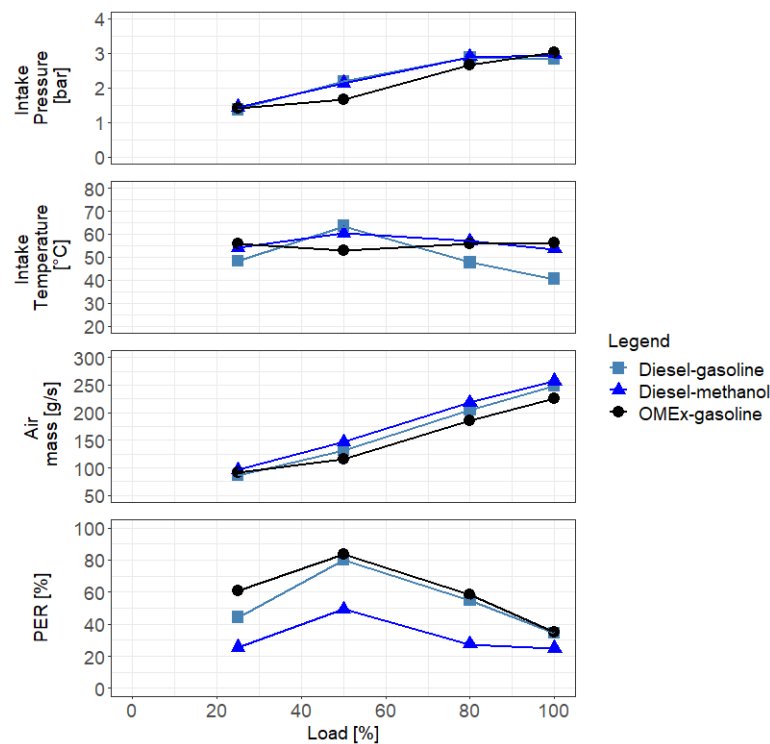
256 The current section discusses the results for each of the different fuel combinations
 257 evaluated. Four engine loads (25%, 50%, 80% and 100%) were tested at 1800 rpm. The
 258 combustion, performance and emissions results are analyzed to grasp the outcome of
 259 the different tested fuels (diesel-methanol and OME_x-gasoline) compared to previously
 260 obtained data for the base case, diesel-gasoline. This is done in order to evaluate the
 261 benefits and drawbacks of replacing gasoline by methanol as LRF and OME_x as HRF, due
 262 to the effect of the different fuel characteristics.

263 3.1. Boundary conditions

264 During the calibration of the operating points, the focus was to achieve the set
 265 targets while respecting the emission constraints (NO_x and soot) and minimizing the
 266 power losses associated to the peripheral systems. Hence, injection pressure, while
 267 being one the parameters that could be adjusted, was always tried to be maintained at

268 the lowest possible value. Nonetheless, when the load increases, the injection pressure
 269 had to be increased to be able to achieve the required amount of fuel in reasonable
 270 injection duration values. Even though, the calibration procedure allowed the intake
 271 conditions to vary between the fuel combinations. As it can be seen in Figure 2, the
 272 differences in terms of air management conditions between fuels are not that high,
 273 being the PER, because its relation to the physical properties of the fuels, the outlier.

274 Diesel-methanol intake pressure values are quite similar to those of diesel-gasoline
 275 for all the operating conditions. However, this fuel combination has a higher air mass
 276 flow (up to 11.5%) due to the cooling effect occurring during the fuel vaporization
 277 because of the higher latent heat of vaporization of methanol. Contrary to this, the air
 278 mass flow for the OMEx-gasoline case shows a reduction of about 6.2% percent with
 279 respect to the diesel-gasoline base case. At medium loads, the intake pressure for
 280 OMEX-gasoline is lower than the other fuel combinations. The higher oxygen content of
 281 OMEx can be attributed as partial responsible for this fact. In addition, since less air mass
 282 flow would be needed to achieve the same oxygen values during the calibration
 283 procedure, the intake pressure can be reduced to minimize the pumping losses, as will
 284 be discussed in further sections.



285
 286 Figure 2. Boundary conditions at the intake manifold.

287

288 Table 5 presents the combustion control parameters that, even if their variations are
 289 not the primary subject of study of this paper, they can have an important effect on the
 290 combustion, performance, and emission characteristics of the tested points. Therefore,
 291 it is of importance to at least take them into consideration when discussing further
 292 results.

293

Table 5. Operating point parameters.

Fuels	Diesel-gasoline				Diesel-methanol				OMEx-gasoline			
Load [%]	25	50	80	100	25	50	80	100	25	50	80	100
Speed [rpm]	1800	1800	1800	1800	1800	1800	1800	1800	1800	1800	1800	1800
EGR [%]	38.1	43.5	35.0	20.4	41.1	38.3	32.8	19.7	38.5	39.7	38.4	33.3
Inj. Pres. [bar]	800	600	2000	2000	800	800	2000	2000	600	600	1200	2000
SOI main [CAD bTDC]	22	50	8	7	16	17	8	11	29	26	10	8
TOI main [μ s]	692	546	889	1323	763	776	1231	1516	952	799	1497	2359
SOI pilot [CAD bTDC]	32	60	-	-	30	32	-	-	44	46	30	-
TOI pilot [μ s]	692	546	-	-	763	776	-	-	952	799	676	-
LRF amount [%]	44.3	79.9	54.8	34.2	42.3	67.3	44.7	41.5	41.0	69.9	38.4	19.5

294

295

3.2. Combustion results

296

297

298

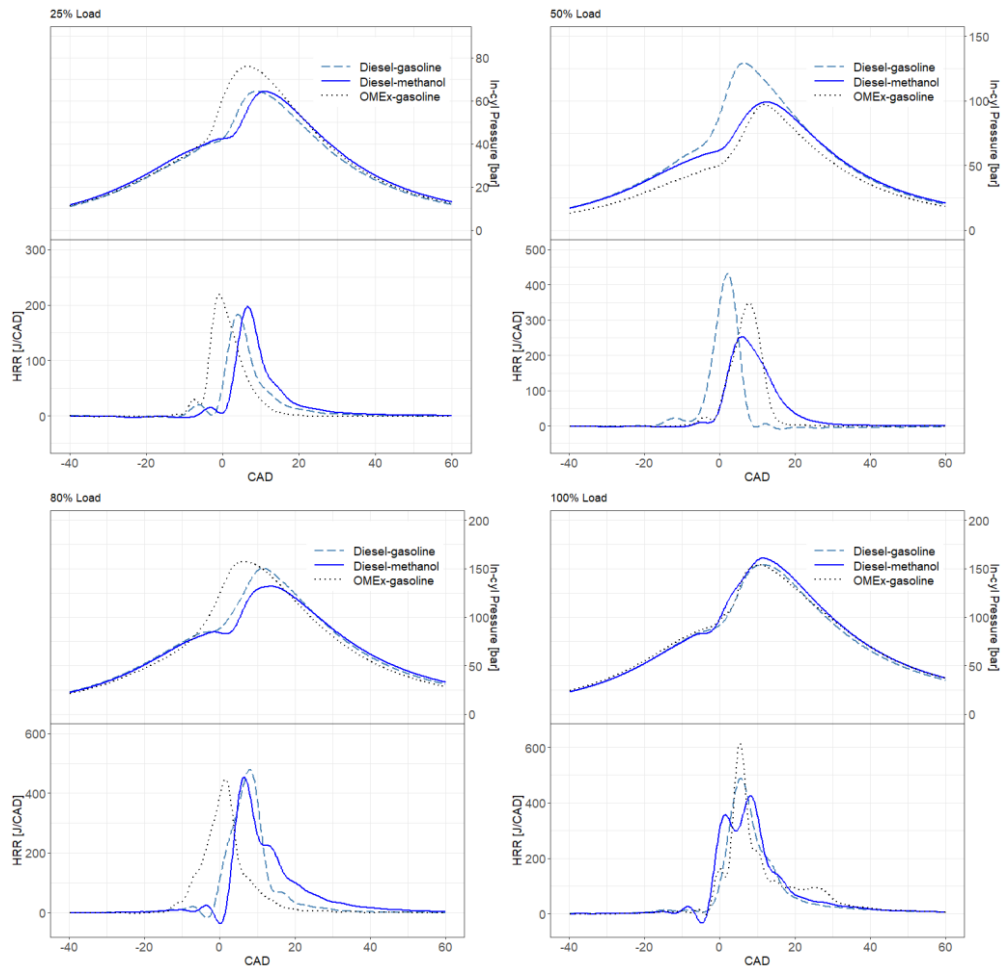
299

300

301

302

Figure 3 shows the comparison of the in-cylinder pressure and heat release rate profiles at all loads for the different fuel combinations tested under the RCCI strategy at 1800 rpm. It is worth mentioning that at low-to-medium load, a fully premixed combustion occurs, while at high-to-full load a dual-fuel diffusive combustion takes place. The analysis will be done by comparing each fuel combination versus the diesel-gasoline reference. This will help to highlight the differences that arise when substituting diesel by OMEx and gasoline by methanol.



303

304

305 Figure 3. Effect of diesel-methanol and OMEx-G on the in-cylinder pressure and heat release rate
 306 for the different operating points.

307 As shown in Figure 3, Diesel-methanol has a delayed combustion from low to high
 308 loads (the phenomenon is reversed at full load), compared to its diesel-gasoline
 309 counterpart. Such a consequence can be assigned to the differences in reactivity
 310 between gasoline and methanol, where gasoline has lower RON and, therefore, the start
 311 of combustion (SOC) takes place early (once the autoignition of the diesel occurs).
 312 Additionally, methanol has a higher RON than gasoline, meaning it can withstand a
 313 bigger compression before igniting. The delayed combustion of the methanol allows
 314 greater time for the fuel mixture once the HRF has been injected, and thus, a more
 315 homogeneous charge is obtained. At full load the trend might be reversed due, in part,
 316 to the tendency to pursue a combustion closer to CDC with multiple injections in order
 317 to be able to avoid the excessive rise rates common of RCCI at high loads [35], and
 318 therefore the combustion is more dependent on the HRF. From low to high loads,
 319 methanol leads to a more advanced SOI_{main} , to supply the necessary energy into the
 320 cylinder and achieve the calibration loads. Methanol used as LRF leads to longer
 321 combustion durations than diesel-gasoline, which is likely to increase the CO production
 322 as will be seen in a later section. This longer combustion can occur due to the lower PER
 323 used with methanol, as was proved by [26]. The 50% burn crank angle (CA50), shown in
 324 figure 4 further reflects the trends seen for the SOC; being interesting to notice how at
 325 full load the diesel-methanol case catches up with the diesel gasoline one. The
 326 explanation for this can be attributed to the more significant role at this load of the HRF.

327 Substituting the gasoline by methanol, a significant reduction of the peak pressure
328 can be seen at medium-to-high loads. This benefit is however not maintained at low and
329 full load. At full load, as was previously stated, the HRF starts playing a more important
330 role on the combustion phasing and characteristics, while at low load the premixed
331 combustion of the lower reactivity methanol promotes in-cylinder pressures that are
332 quite similar or smaller than those found with gasoline. As will be seen in further
333 sections, methanol is conducive to a reduction of the maximum pressure gradient,
334 precisely because of that reduced reactivity.

335 PERs are lower for diesel-methanol because methanol has a significantly lower LHV than
336 gasoline. This, in turn, can cause a reduction of the maximum in-chamber temperature
337 [36], phenomenon that occurred for all the operating points using diesel-methanol,
338 except the 100% load. These low PER values lead to a larger diffusive phase of the
339 combustion especially at 25% and 80% loads, as shown in Figure 3.

340 OME_x presents important changes in LHV and reactivity compared to diesel (it has a
341 lower LHV and a higher cetane number). The higher cetane number promotes in-cylinder
342 local fuel mixtures with higher cetane number than diesel, which helps to reduce the
343 combustion delay, as shown in the cases of 25% and 80% load. Moreover, it is useful to
344 highlight that at 25% load the higher reactivity of OME_x results in shorter combustion
345 duration, as can be appreciated in Figure 4. The heat release rate for this load shows a
346 low temperature heat release (LTHR) (as does as well the 50% load operating condition).
347 Contrarily, for the other loads, as the HRF becomes more predominant in the
348 combustion phasing, the combustion duration of OME_x is longer, despite having a higher
349 fuel reactivity, because it has a lower LHV than diesel. The 50% load condition is unusual
350 in that an important delay of the start of combustion is observed. It is considered that
351 this effect is originated by the lower heating value and the requirement of bigger fuel
352 quantities to achieve the necessary energy for the combustion. Another result of the
353 properties changes of OME_x is that its injection rates are considerably longer to achieve
354 the energy levels necessary to reach the load conditions.

355 The full and 50% load cases do not present increases regarding the in-cylinder
356 pressure curve against the diesel-gasoline one. In fact, the maximum pressure is almost
357 the same at full load and is lower by 24.8% at medium load. Notwithstanding, low and
358 medium-high load are comprised of increments of 18% and 3.7%, respectively.

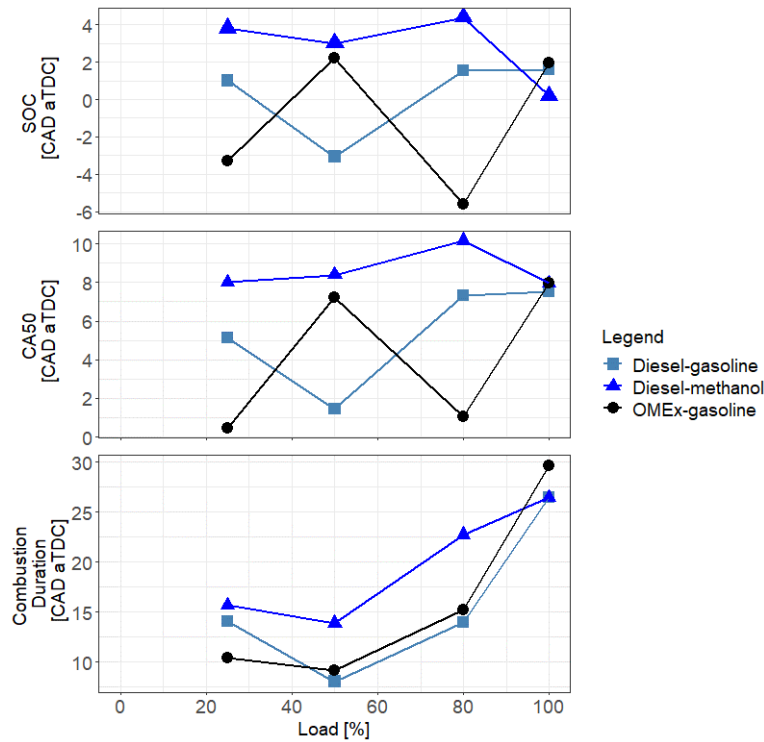
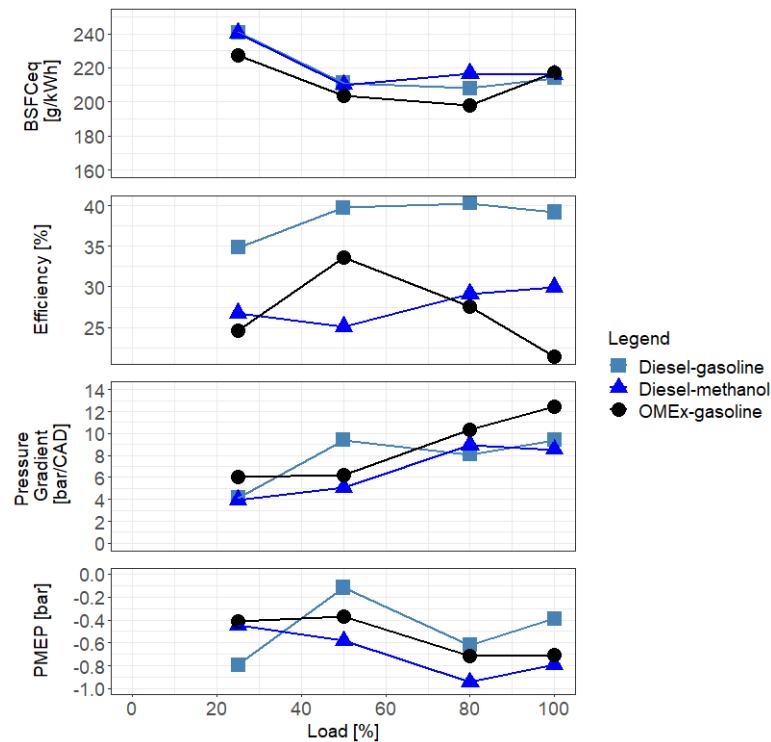


Figure 4. Effect of diesel-methanol and OME-gasoline on the start of combustion and combustion duration.

3.3. Performance results

The calibration process used was intended, among other objectives, to reduce the unacceptable pressure rise rates and peak cylinder pressures that can potentially damage the engine or cause excessive noise. This section evaluates the performance results of the studied fuels to evaluate its advantages and disadvantages. As shown in Figure 5, at low-to-medium load, diesel-methanol presents slight reductions in $BSFC_{eq}$, specifically 0.16% and 0.42%, as well as lower pressure gradients. In this sense, the octane number is a feasible cause since a higher value for the number indicates that methanol can be compressed further without igniting, acting as a damping property of the pressure rise rate (PRR). The reduction of the PRR is in agreement with prolonged combustion duration and is a desirable feature to reduce the mechanical damage and increased engine noise. PMEP for diesel-methanol is 0.35 bar over the diesel-gasoline calibration at the lowest load tested; this trend is reversed at higher loads, but the methanol-originated pumping losses do not add demand for additional turbocharger requirements. From Figure 5, it can be seen that using methanol has lower efficiency than gasoline, but recalling the huge difference of LHV that these two fuels possess can explain this phenomenon, as gasoline has a bigger energetic content. In terms of fuel consumption, it is seen that for both cases, substituting a fuel from the diesel-gasoline base case carries some fuel consumption penalties (around 40% more). By this reason, the fuel consumption was compared in terms of $BSFC_{eq}$, as explained in section 2.4, to exclude the effect of the LHV and compare the fuels by their fuel conversion efficiency instead of just the amount of fuel. Then, it can be said that OME produces an important decrease in $BSFC_{eq}$, since its energy conversion seems to prove to be better. On, non-equivalent, BSFC criteria, the OME is up to 176 g/kWh higher than the diesel case. OME also shows elevated pressure gradients compared to diesel-gasoline and diesel-

387 methanol, which can be attributed to the higher reactivity of the fuel. OME_x has higher
 388 pumping losses than diesel-methanol, but lower than diesel-gasoline as the required
 389 pumping mean effective pressure is lower. This coincides with findings reported in
 390 [16]. The efficiency of the OME_x-gasoline case is inferior to that of diesel-gasoline, which
 391 can be appointed to the smaller LHV of OME_x and the reduction of the engine power,
 392 which is a direct consequence of its higher oxygen content [37]; the same assumption
 393 can be made for methanol. As with diesel-methanol, PMEP values are lower with OME_x,
 394 however this change is not as significant as with methanol.



395

396

397

Figure 5. Effect of diesel-methanol and OME_x-G on performance parameters: BSFC_{eq}, Efficiency, Pressure Gradient and PMEP.

398

3.4. Emission results

399

400

401

402

403

404

405

406

407

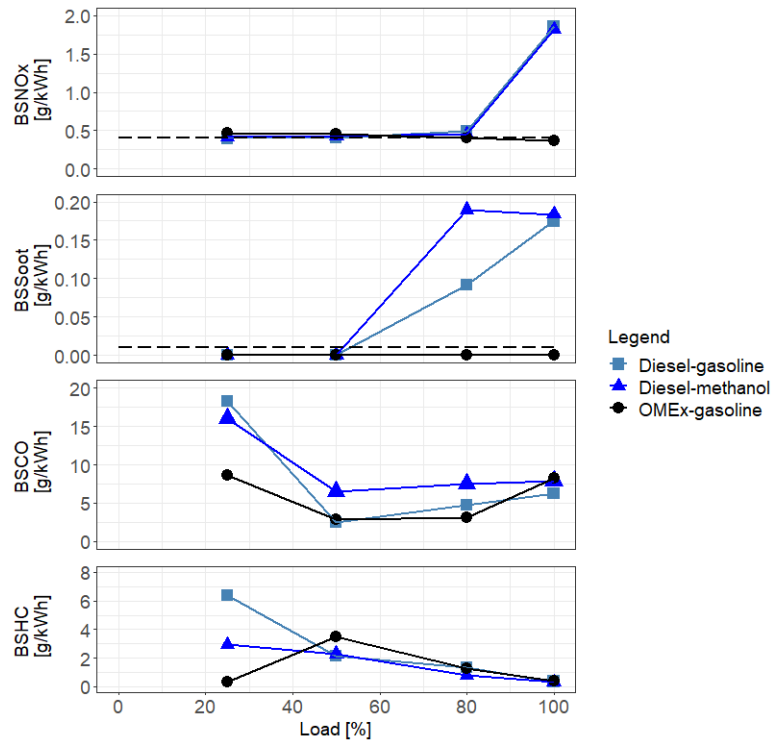
408

409

410

411

Regarding the emission parameters shown in Figure 6, the diesel-methanol blend results in increased NO_x emissions for all the low-to-medium load operating conditions compared to the diesel-gasoline operation. On this point, is important to highlight that these values are very close to the EURO VI limits, so even though the values for methanol are higher, the difference does not exceed 0.05 g/kWh above the EURO VI limit. The extended combustion duration discussed in section 3.2 increases the residence time at high temperatures, crucial factor in the thermal mechanism of NO_x formation. At full load, the NO_x emissions levels from the diesel-methanol operation are lower by 2%. This reduction in NO_x can be due to the fact that at higher loads, the combustion is more heavily influenced by the HRF which for both the base case (diesel-gasoline) and the diesel-methanol case is diesel. Hence, this slight difference in emissions could be a combination of different factors and not a direct consequence of the fuel used, since diesel is the fuel that governs both combustion conditions at this load.



412

413

414

Figure 6. Effect of diesel-methanol and OMEx-G on emissions parameters: BSNOx, BSSoot, BSCO and BSHC.

415

416

417

418

419

420

421

422

423

424

425

426

HC emissions for diesel-methanol are similar to that of diesel-gasoline, at medium-to-full load, because of the reduction of premixing. So, even although the combustion duration is longer for the methanol, its late combustion timing balances out the effect of the residence times, thus allowing the reduction of incomplete combustion. The low load condition completely inverts this trend, with diesel methanol having over 6 g/kWh of unburned HC more than diesel-gasoline. Soot emissions are higher, mainly at 80% of engine load. This is somewhat counter-intuitive since the methanol has higher oxygen content than gasoline and that is expected to reduce soot formation. Then, other possible factors that can influence soot formation must be inspected, being the PER and the reduced percentage of LRF good candidates to explain this. To further explain the previous point, the percentage of methanol injected through the PFI, and its low soot properties, are not enough to counterbalance the effects of the soot formation.

427

428

429

430

431

432

433

434

435

436

437

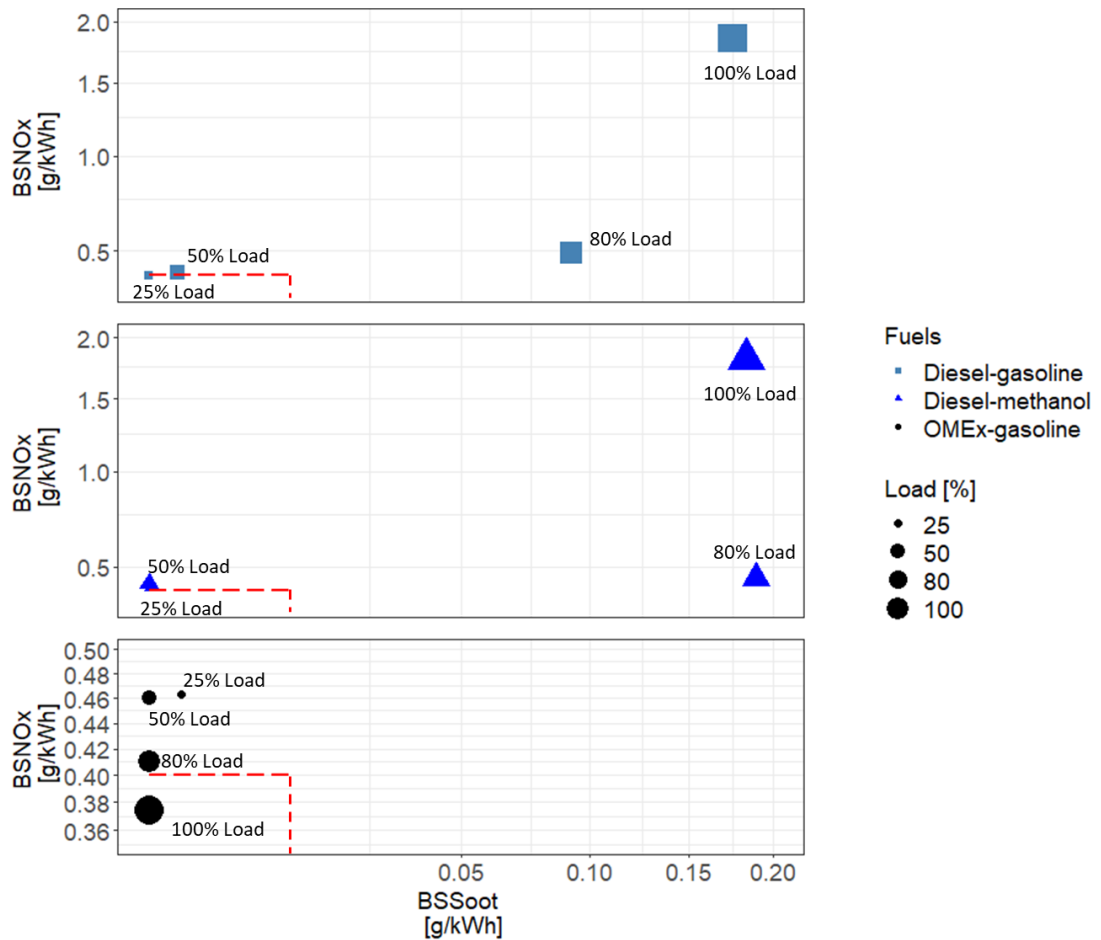
438

439

The NOx emissions tend to increase as the ignition advances, which is the case for the medium-to-low load conditions for the OMEx-gasoline. However, the NOx values product of the calibration procedure remain close to the EURO VI limits. This is consequence of that the OMEx burning produces virtually no soot emissions due to the high oxygen concentration. Therefore, the air management system can be controlled to provide the adequate EGR levels to inhibit the NOx pollutants formation. Even at full load, where the diesel-gasoline exceeds by far the legislation limits, the OMEx values remained under it. Additionally, OMEx has a higher cetane number, which allows a higher power output [38], thus, it is possible to reach the required load with lower NOx and soot emission than diesel-gasoline. At full load, a counter effect of the lower NOx is an increase of unburned HCs, but compared to the NOx improvement is quite small (0.06 g/kWh). The 50% load also shows more elevated HCs than the diesel-diesel gasoline case, and 0.05 g/kWh more of NOx emissions. For the remaining loads, the HC emissions

440 are lower with OMEx. CO emissions for medium-to-full load are quite similar to diesel-
 441 methanol, while at 25% load a reduction of 9.7 g/kWh is observed.

442 **3.5. Fuel evaluation for EURO VI**
 443



444
 445 Figure 6. NOx-soot trade-off for diesel-gasoline, diesel-methanol and OMEx-gasoline fuel blends.
 446 Left: All points. Right: Points that achieve soot limitations.

447 Conventionally, the NOx-soot tradeoff is one of the difficult challenges to face when
 448 trying to optimize ICEs to comply with regulations. Figure 6 shows the emissions
 449 commented in section 3.4, plotted in trade-off format to highlight more clearly the
 450 benefits of each fuel against the other. From Figure 6 it is evident that OMEx-gasoline
 451 has the best NOx-soot tradeoff, since it is the only fuel combination for which, at least, all
 452 the operating points at all the loads have soot values under 0.01 g/kWh.

453 To further confirm the advantages and disadvantages of the fuel blends they were
 454 weighted against each other by means of the following function:

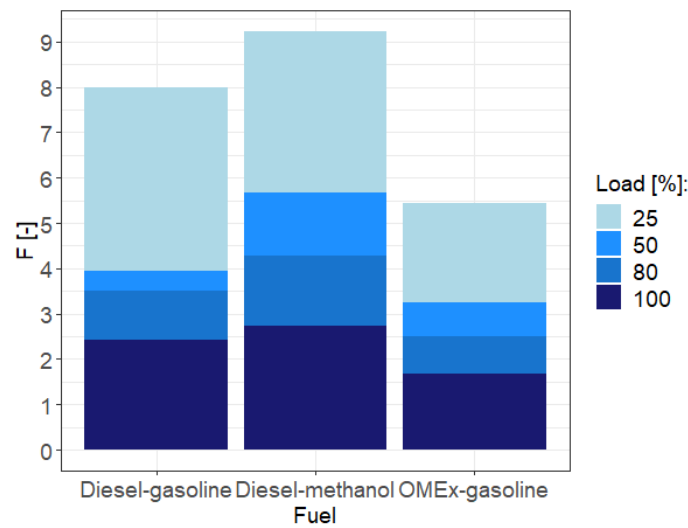
$$F = \sum \frac{X - X_{limit}}{X_{max} - X_{min}} \quad (2)$$

455 Where X represents the parameters to be evaluated (BSFC_{eq}, BSNOx, BSSoot, BSCO,
 456 BSHC); X_{limit} is the maximum value allowed by regulations or in the case of BSFC_{eq} the
 457 value for diesel-gasoline; X_{max} is the maximum value for the parameter in the dataset

458 and X_{min} the minimum one. Emissions have been normalized with respect to EURO VI
 459 limits and BSFC_{eq} by the aforementioned diesel-gasoline case.

460 Figure 7 illustrates the total sum of the penalization of each parameter evaluated for
 461 each fuel combination. The distribution of this penalizations by load is also
 462 distinguishable. The smaller the value of F , the closer the fuel combination is to ideal
 463 fuel and emissions performance. Then, it is evident that OMEx-gasoline is the fuel
 464 combination that better satisfies the trade-off between emissions and BSFC_{eq}. While
 465 diesel-methanol seems to perform the worst under the selected criterion, from sections
 466 3.2 to 3.4 and previous research [26] is important to recall that it possesses
 467 characteristics that can help to achieve combustion targets and that could improve its
 468 desirability as a fuel when performing a complete life cycle analysis. Thus, more research
 469 on the fuel is recommended.

470



471

Figure 7. Penalization of the different fuel combinations by load.

472

3.6. Potential of OMEx to reach potential EURO VII conditions

473

474 As shown in the previous subsection, the advantages of substituting diesel by OMEx
 475 surpass the advantages of replacing the gasoline by methanol. This inspired further
 476 testing with the OMEx-gasoline combination. More specifically, an EGR sweep was
 477 performed in order to assess whether or not OMEx has the potential to fulfill the EURO
 478 VI emissions limitation for both NO_x and soot emissions simultaneously -and even the
 potential EURO VII- without the need for after-treatment systems (ATS).

479

480 The tests were performed with constant parameters at 10, 25, 50, 75 and 100% loads
 481 to successfully isolate the effect of EGR on the combustion. In order to keep the total
 482 admitted mass constant, the turbine was set to turn together with low pressure and high
 pressure EGR. The respective settings are described in Table 6.

483

Table 6. Constant parameter for characterization of the effect of EGR on OMEx-gasoline.

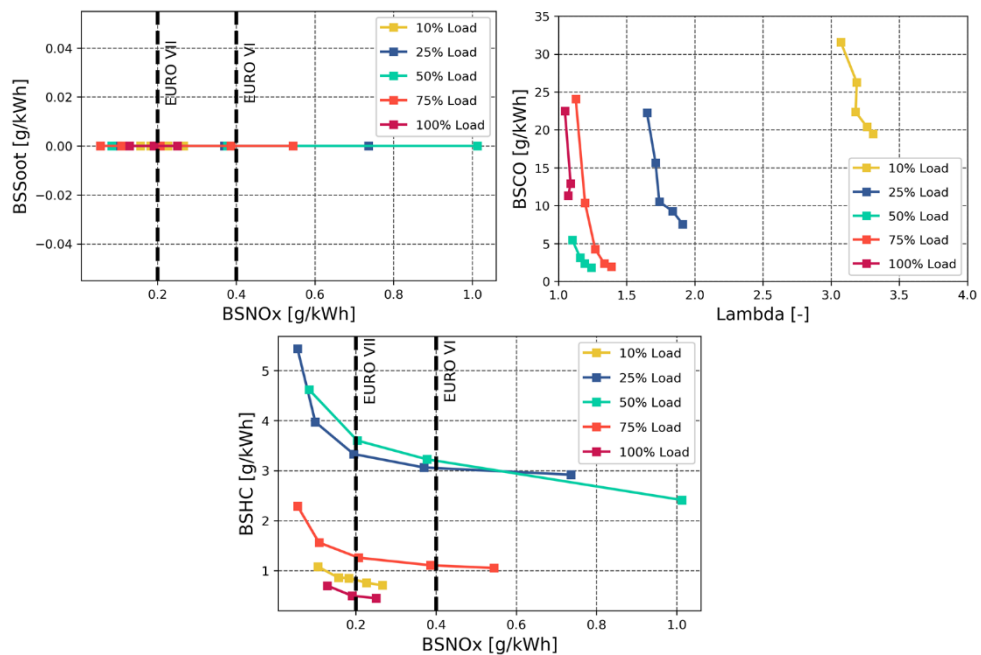
	PER [%]	Pintake [bar]	Madm [g/s]	Mfuel [g/s]	SOI main [CAD bTDC]	SOI pilot [CAD bTDC]
10%	0	1.19	133	5.37	6	22

25%	59.8	1.38	154	6.5	29	44
50%	83.6	1.66	191	8.5	26	46
75%	58.3	2.66	287	15.9	10	30
100%	34.8	3.03	330	27.6	8	-
Max. dev.	±0.5	±0.01	±3	±0.1	-	-

484

485 The most straight forward solution to reduce the NOx production in the ICEs is the
486 use of EGR. However, it is necessary to confirm if this effect is achieved without a great
487 impact on the other emissions. Since more EGR reduces the in-cylinder temperature,
488 inhibiting the oxidation reactions, a consequent increase for the HC and CO emissions is
489 expected. As seen in Figure 8, in the case of OMEx, the impact of the EGR on the trade-
490 off for NOx-HC and NOx-CO can be considered important (an increase of 2.5 g/kWh of
491 HC for 0.7 g/kWh of NOx reduced for the former and 20 g/kWh of CO for 0.5 g/kWh
492 reduced in NOx for the latter) the negligible effect the EGR increase generates on soot
493 formation makes OMEx a formidable fuel to reach the emissions restriction levels.
494 Furthermore, Figure 9 shows that increasing the EGR rate delays the combustion and
495 increases the combustion duration. The delayed CA50 is the main cause of reduction of
496 the engine torque.

497

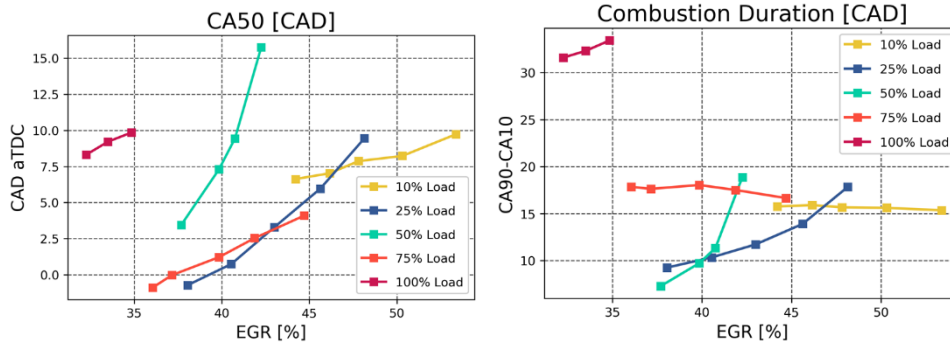


498

499

500

Figure 8. Engine emissions tradeoff during the EGR exploration tests. Top: BSSoot-BSNOx trade-off. Left: BSFCO-BSNOx trade-off. Right: BSCH-BSNOx trade-off.



501

502

Figure 9. Combustion performance trade-off during the EGR exploration.

503

504

505

506

507

508

509

Figure 10 shows how increasing the EGR to reduce NO_x formation also reduces the effective torque of the engine, thus affecting the fuel consumption. From the same Figure, it can be appreciated how going from EURO VI to the potential EURO VII has minimal effects on torque. Additionally, the increase on BSFC_{eq} is still affordable as it does not surpass a 10% increase in the most critical case. Greater reductions than the potential EURO VII in NO_x will penalize greatly the specific fuel consumption, as the injected fuel mass will have to increase to keep torque.

510

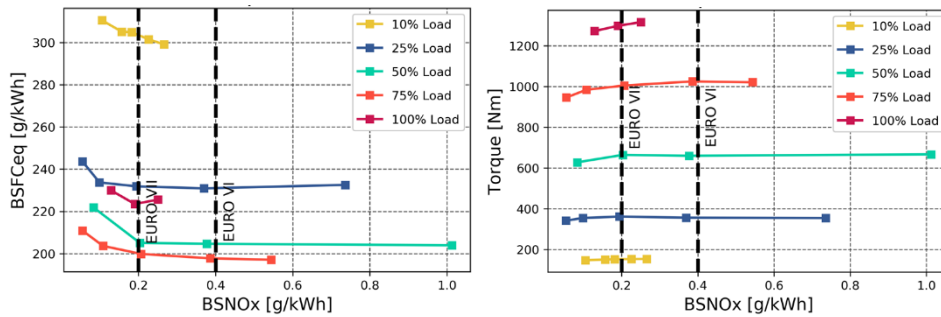
511

512

513

514

Finally, after evaluating of the conditions at the exhaust, it is apparent that the use of an ATS becomes necessary with the increase of the previously mentioned HC and CO emissions. Regarding the possible performance of this device, its acknowledged that it might be reduced due to the low exhaust oxygen concentration and high exhaust temperature.

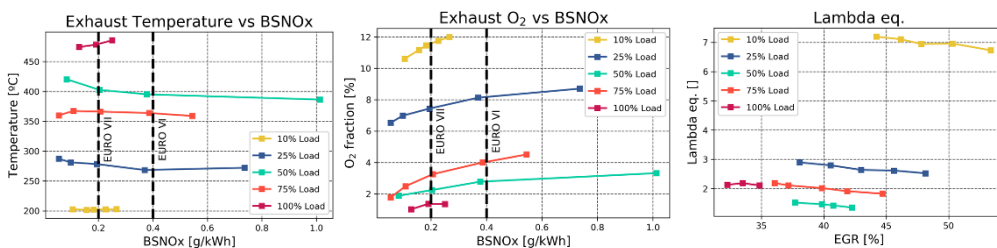


515

516

517

Figure 10. Engine performance tradeoff during the EGR exploration. Left: BSFCeq-BSNOx tradeoff. Right: Torque-BSNOx trade-off.



518

519

Figure 11. Exhaust boundary conditions at low NO_x conditions.

520

4. Conclusions

521

522

This work discussed the potential of a DMDF operated engine towards the potential EURO VII emissions regulation compliance testing both diesel-methanol and OMe_x-

523 gasoline. As a first step, the combustion was evaluated following a dedicated calibration
524 at 1800 rpm and four different load levels for both fuel combinations tested, and
525 comparing them in terms of combustion, performance and emissions to a base diesel-
526 gasoline case under the same conditions. From this, the most relevant highlight are:

- 527 • Diesel-methanol DFDM has similar emissions performance as the diesel-
528 gasoline base case in terms of NO_x and HC because combustion is highly
529 dependent on the HRF, which is diesel for both cases.
- 530 • Soot and CO emissions increase, when operating with diesel-methanol,
531 except at 25 % load, where soot is equal, and CO is reduced by 12%.
- 532 • The use of diesel-methanol has minimal effects regarding BSFC_{eq}; however,
533 fuel consumption is increased significantly because the lower LHV of
534 methanol has to be compensated by injecting more diesel fuel and reaching
535 a lower PER and LRF percentage to keep emissions under control.
- 536 • By using methanol, the mechanical integrity of the engine improves as the
537 slower combustion of methanol produces lower pressure gradients and
538 pressure peaks.
- 539 • The results for OMEx paint a better picture in terms of compliance with Euro
540 VI regulations. When comparing the performance of the fuel against diesel-
541 gasoline, it showed a reduction of NO_x for the high-to-full load. Especially at
542 full load, the reduction of NO_x is 79.8% (from 1.85 g/kWh with diesel-gasoline
543 to 0.37 g/kWh with OMEX-gasoline), more so, results do not exceed 0.46
544 g/kWh of NO_x for the fuel combination.
- 545 • OMEx-gasoline soot production is the lowest of all the fuel combinations
546 tested in this research.
- 547 • The use of OMEx instead of diesel generates BSFC increases of up to 176
548 g/kWh, when not compared in equivalent terms. The requirement of more
549 fuel than its counterpart derives from its lower LHV. On the flipside, BSFC_{eq}
550 is lower for OMEx-gasoline for all loads but the 100% load, indicating a good
551 energy conversion ratio.

552 From the first stage, after evaluating the superior performance of OMEx in the
553 reduction of soot, an EGR sweep test was performed to evaluate the capabilities of
554 reducing NO_x emissions using OMEx and the impact on the other emissions and
555 performance characteristics. It was found that:

- 556 • The OMEx-gasoline DFDM can accomplish reaching the potential EURO VII
557 NO_x levels (BSNO_x=0.2g/kWh) and still be considered inside the low impact
558 region of the tradeoff with BSFC and other regulated emissions.
- 559 • OMEx does have bigger CO and HC emissions than diesel-gasoline. This
560 increase of CO and HC emissions makes necessary the use of an ATS, but
561 depletion of oxygen at the exhaust may be a problem for its operation.
- 562 • The OMEx-gasoline blend produces virtually no soot; even at high EGR values
563 because of its high oxygen content. This fact, in turn allows the reduction of
564 pumping losses because the air management system can be calibrated
565 without generating soot emissions above the imposed limit.

566 Finally, it can be concluded that the DMDF concept paired with relatively new fuels such
567 as OMEx can help bridge the gap between the current state of ICEs and regulated

568 emissions, even up to the potential EURO VII for NO_x. However, OME_x-gasoline has
569 drawbacks that must be addressed before reaching the points of commercial availability,
570 i.e. the higher CO and HC emissions coupled with reduced possible operability of an ATS.
571 Future work might be an important tool to understand how to better solve these issues.

572 **Acknowledgments**

573 The authors thanks ARAMCO Overseas Company and VOLVO Group Trucks Technology
574 for supporting this research. The authors acknowledge FEDER and Spanish Ministerio de
575 Economía y Competitividad for partially supporting this research through TRANCO
576 project (TRA2017-87694-R). The authors also acknowledge the Universitat Politècnica
577 de València for partially supporting this research through Convocatoria de ayudas a
578 Primeros Proyectos de Investigación (PAID-06-18).

579 **References**

580

- [1] S. Broitman and B. A. Portnov, "Forecasting health effects potentially associated with the relocation of a major air pollution source," *Environmental Research*, p. 109088, 2020.
- [2] G. I., B. C., L. Lanza and P. La Barbera, "Storm water pollution in the urban environment of Genoa, Italy," *Atmospheric Research*, vol. 77, no. 1-4, pp. 60-73, 2005.
- [3] E. Commission, "European Commission," European Union, 2020. [Online]. Available: https://ec.europa.eu/clima/policies/transport_en. [Accessed 6 June 2020].
- [4] W. J. Requia, M. Mohamed, C. D. Higgins, A. Arain and M. Ferguson, "How clean are electric vehicles? Evidence-based review of the effects of electric mobility on air pollutants, greenhouse gas emissions and human health," *Atmospheric Environment*, vol. 185, pp. 64-77, 2018.
- [5] G. Kalghatgi, "Is it really the end of internal combustion engines and petroleum in transport?," *Applied Energy*, vol. 225, pp. 965-974, 2018.
- [6] V. Karthickeyan, "Effect of combustion chamber bowl geometry modification on engine performance, combustion and emission characteristics of biodiesel fuelled diesel engine with its energy and exergy analysis," *Energy*, vol. 176, pp. 830-852, 2019.
- [7] H. Kim and S. Song, "Concept design of a novel reformer producing hydrogen for internal combustion engines using fuel decomposition method: Performance evaluation of coated monolith suitable for on-board applications," *International Journal of Hydrogen Energy*, vol. 45, no. 16, pp. 9353-9367, 2020.
- [8] J. Benajes, A. García, J. Monsalve-Serrano and R. Sari, "Fuel consumption and engine-out emissions estimations of a light-duty engine running in dual-mode RCCI/CDC with different fuels and driving cycles," *Energy*, vol. 157, pp. 19-30, 2018.
- [9] V. Macián, V. Bermúdez, D. Villalta and L. Soto, "Effects of low-pressure EGR on gaseous emissions and particle size distribution from a dual-mode dual-fuel (DMDF) concept in a medium-duty engine," *Applied Thermal Engineering*, vol. 163, p. 114245, 2019.

- [10] J. M. Luján, A. García, J. Monsalve-Serrano and S. Matínez-Boggio, "Effectiveness of hybrid powertrains to reduce the fuel consumption and NOx emissions of a Euro 6d-temp diesel engine under real-life driving conditions," *Energy Conversion and Management*, vol. 199, p. 111987, 2019.
- [11] P. Di Giorgio, P. Di Trolio, M. Minutillo and F. V. Conte, "Model based preliminary design and optimization of Internal Combustion Engine and Fuel Cell hybrid electric vehicle," *Energy Procedia*, vol. 148, pp. 1191-1198, 2018.
- [12] J. Wei, Y. Zeng, M. Pan, Y. Zhuang, L. Qiu, T. Zhou and Y. Liu, "Morphology analysis of soot particles from a modern diesel engine fueled with different types of oxygenated fuels," *Fuel*, vol. 267, p. 117248, 2020.
- [13] J. Han, S. Wang, R. M. Vittori and S. L.M.T., "Experimental study of the combustion and emission characteristics of oxygenated fuels on a heavy-duty diesel engine," *Fuel*, vol. 268, p. 117219, 2020.
- [14] L. Cai, S. Jacobs, R. Langer, F. vom Lehn, K. A. Heufer and H. Pitsch, "Auto-ignition of oxymethylene ethers (OMEn, n = 2–4) as promising synthetic e-fuels from renewable electricity: shock tube experiments and automatic mechanism generation," *Fuel*, vol. 264, p. 116711, 2020.
- [15] H. Jiang, L. Wei, X. Fan, J. Xu, W. Shyy and T. Zhao, "A novel energy storage system incorporating electrically rechargeable liquid fuels as the storage medium," *Science Bulletin*, vol. 64, no. 4, pp. 270-280, 2019.
- [16] J. Benajes, A. García, J. Monsalve-Serrano and R. Sari, "Clean and efficient dual-fuel combustion using OMEx as high reactivity fuel: Comparison to diesel-gasoline calibration," *Energy Conversion and Management*, vol. 216, p. 112953, 2020.
- [17] X. Wang, C. Cheung, Y. Di and Z. Huang, "Diesel engine gaseous and particle emissions fueled with diesel–oxygenate blends," *Fuel*, vol. 94, pp. 317-323, 2012.
- [18] J. Abboud, J. Schobing, G. Legros, J. Bonnetty, V. Tschamber, A. Brillard, G. Leyssens, V. Lauga, E. E. Iojoiu and P. Da Costaa, "Impacts of oxygenated compounds concentration on sooting propensities and soot oxidative reactivity: Application to Diesel and Biodiesel surrogates," *Fuel*, vol. 193, pp. 241-253, 2017.
- [19] C. Yao, W. Pan and A. Yao, "Methanol fumigation in compression-ignition engines: A critical review of recent academic and technological developments," *Fuel*, vol. 209, pp. 713-732, 2017.
- [20] S. Verhelstab, J. W. Turnerc, L. Sileghemb and J. Vancoillieb, "Methanol as a fuel for internal combustion engines," *Progress in Energy and Combustion Science*, vol. 70, pp. 43-88, January 2019.
- [21] G. Labeckas, S. Slavinskas and I. Kanapkienė, "The individual effects of cetane number, oxygen content or fuel properties on the ignition delay, combustion characteristics, and cyclic variation of a turbocharged CRDI diesel engine – Part 1," *Energy Conversion and Management*, no. 148, pp. 1003-1027, 2017.

- [22] P. Hellier, M. Talibi, A. Eveleigh and N. Ladommatos, "An overview of the effects of fuel molecular structure on the combustion and emissions characteristics of compression ignition engines," *Proceedings of the Institution of Mechanical Engineers, Part D: Journal of Automobile Engineering*, vol. 232, no. 1, pp. 90-105, 2018.
- [23] Z. Huang, H. Lu, D. Jiang, K. Zeng, B. Liu, J. Zhang and X. Wang, "Combustion behaviors of a compression-ignition engine fuelled with diesel/methanol blends under various fuel delivery advance angles," *Bioresource Technology*, vol. 95, no. 3, pp. 331-341, 2004.
- [24] H. Bayraktar, "An experimental study on the performance parameters of an experimental CI engine fuelled with diesel–methanol–dodecanol blends," *Fuel*, vol. 87, pp. 158-164, 2008.
- [25] Y. Li, M. Jia, L. Xu and X.-S. Bai, "Multiple-objective optimization of methanol/diesel dual-fuel engine at low loads: A comparison of reactivity controlled compression ignition (RCCI) and direct dual fuel stratification (DDFS) strategies," *Fuel*, vol. 262, p. 116673, 2020.
- [26] G. Duraisamy, Rangasamy and N. Govindan, "A comparative study on methanol/diesel and methanol/PODE dual fuel RCCI combustion in an automotive diesel engine," *Renewable Energy*, vol. 145, pp. 542-556, 2020.
- [27] Z. Jia and I. Denbratt, "Experimental investigation into the combustion characteristics of a methanol-Diesel heavy duty engine operated in RCCI mode," *Fuel*, vol. 226, pp. 745-753, 2018.
- [28] S. Iannuzzi, C. Barro, K. Boulouchos and J. Burger, "Combustion behavior and soot formation/oxidation of oxygenated fuels in a cylindrical constant volume chamber," *Fuel*, vol. 167, pp. 49-59, 2016.
- [29] J. Benajes, A. García, J. Monsalve-Serrano and S. Martínez-Boggio, "Potential of using OME_x as substitute of diesel in the dual-fuel combustion mode to reduce the global CO₂ emissions," *Transportation Engineering*, vol. 1, p. 100001, 2020.
- [30] D. Oestreich, L. Lautenschütz, U. Arnold and J. Sauer, "Production of oxymethylene dimethyl ether (OME)-hydrocarbon fuel blends in a one-step synthesis/extraction procedure," *Fuel*, no. 214, pp. 39-44, 2017.
- [31] J. Benajes, A. García, J. Monsalve-Serrano and R. Sri, "Clean and efficient dual-fuel combustion using OME_x as high reactivity fuel: Comparison to diesel-gasoline calibration," *Energy Conversion and Management*, vol. 216, p. 112953, 2020.
- [32] A. García, J. Monsalve-Serrano, D. Villalta, R. Sari, V. G. Zavaleta and P. Gaillard, "Potential of e-Fischer Tropsch diesel and oxymethyl-ether (OME_x) as fuels for the dual-mode dual-fuel concept," *Applied Energy*, vol. 253, p. 113622, 2019.
- [33] A. García, A. Gil, J. Monsalve-Serrano and R. Lago Sari, "OME_x-diesel blends as high reactivity fuel for ultra-low NO_x and soot emissions in the dual-mode dual-fuel combustion strategy," *Fuel*, vol. 275, p. 117898, 2020.

- [34] AVL, *AVL manufacturer manual. Smoke value measurement with the filter-paper method. Application notes.*, 2005.
- [35] S. Molina, A. García, J. Pastor and E. Belarte, "Operating range extension of RCCI combustion concept from low to full load in a heavy-duty engine," *Applied Energy*, vol. 143, pp. 211-227, 2015.
- [36] W. Han, Y. Lu, C. Jin, X. Tian, Y. Peng, S. Pan, H. Liu, P. Zhang and Y. Zhong, "Study on influencing factors of particle emissions from a RCCI engine with variation of premixing ratio and total cycle energy," *Energy*, vol. 202, p. 117707, 2020.
- [37] E. Sendžikienė, V. Makareviciene and P. Janulis, "Influence of fuel oxygen content on diesel engine exhaust emissions," *Renewable Energy*, vol. 31, no. 15, pp. 2505-2512, 2006.
- [38] R. Li, Z. Wang, P. Ni, Y. Zhao, M. Li and L. Li, "Effects of cetane number improvers on the performance of diesel engine fuelled with methanol/biodiesel blend," *Fuel*, vol. 128, pp. 180-187, 2014.
- [39] S. Han, J. Kim and C. Bae, "Effect of air-fuel mixing quality on characteristics of conventional and low temperature diesel combustion," *Applied Energy*, vol. 119, pp. 454-466, 2014.
- [40] S. L. Plee, T. Ahmand and M. J. P., "Flame temperature correlation for the effects of exhaust gas recirculation on diesel particulate and NOx emissions," *SAE Transactions*, vol. 90, pp. 3738-3754, 1981.

581

582

583 **Abbreviations**

584 ATDC: After Top Dead Center

585 ATS: After Treatment System

586 BSFC_{eq}: Equivalent Brake Specific Fuel Consumption

587 BTDC: Before Top Dead Center

588 CAD: Crank Angle Degree

589 CDC: Conventional Diesel Combustion

590 CO: Carbon Monoxide

591 CO₂: Carbon Dioxide

592 DDFS: Direct dual fuel stratification

593 DI: Direct Injection

594 DMDF: Dual Mode Dual Fuel

595 EGR: Exhaust Gas Recirculation

596 FIS: Fuel Injection System
597 FSN: Filter Smoke Number
598 HC: Hydrocarbons
599 HRR: Heat Release Rate
600 HRF: High Reactivity Fuel
601 IMEP: Indicated Mean Effective Pressure
602 LRF: Low Reactivity Fuel
603 LTC: Low Temperature Combustion
604 LTHR: Low Temperature Heat Release
605 LHV: Lower Heating Value
606 NOx: Nitrogen Oxides
607 OME_x: Oxymethylene Ether
608 PER: Premix Energy Ratio
609 PMEP: Pumping Mean Effective Pressure
610 PFI: Port Fuel Injection
611 RCCI: Reactivity Controlled Compression Ignition
612 RON: Research Octane Number
613 SOI: Start of Injection
614 TDC: Top Dead Center
615 MON: Motor Octane Number
616 VGT: Variable Geometry Turbine
617 WHVC: Worldwide Harmonized Vehicle Cycle